

Dynamics of the charge-density-wave mode in $(\text{NbSe}_4)_2\text{I}$

A. Philipp and W. Mayr

*Institut für Festkörperphysik der Universität Wien, Vienna, Austria
and Ludwig Boltzmann Institut für Festkörperphysik, Vienna, Austria*

T. W. Kim, B. Alavi, M. Maki, and G. Grüner

Department of Physics and Solid State Science Center, University of California, Los Angeles, California 90024

(Received 12 October 1988)

We have measured the ac response in the radiofrequency-to-millimeter-wave spectral range in the compound $(\text{NbSe}_4)_2\text{I}$, which undergoes a transition to a charge-density wave below room temperature. The pinned-mode resonance appears around 35 GHz, and it is analyzed assuming a simple harmonic-oscillator model. The temperature dependences of the parameters, the effective mass m^* , pinning frequency ω_0 , and damping constant τ^* are extracted, and their temperature dependence compared with the various theories. The response well below the pinning frequency in the radiofrequency spectral range is analyzed assuming a phenomenological expression for both $\text{Re}\sigma$ and $\text{Im}\sigma$, used earlier for other materials in their charge-density-wave states. In contrast to a temperature-independent pinning frequency, both the low-frequency dielectric constant ϵ and the threshold field for the nonlinear conduction E_T are strongly temperature dependent, with ϵE_T approximately constant. The observed features are also contrasted with results obtained on other materials in their charge-density-wave states.

I. INTRODUCTION

Various aspects of charge-density-wave (CDW) conduction have been explored by a range of experimental techniques which focus on the nonlinear and/or frequency-dependent response of the ground-state condensate.¹ Central to the ac response is the notion of CDW pinning by impurities and lattice imperfections. This leads to the shift of the oscillator strength from zero to finite frequencies. Damping associated with the dynamics of the collective mode leads, together with possible disorder effects, to a broadening of the spectral response, while the total oscillator strength is determined by the effective mass m^* of the ground state. The above features have been examined in the model compounds TaS_3 ,² $(\text{TaSe}_4)_2\text{I}$,³ and $\text{K}_{0.3}\text{MoO}_3$,⁴ which have semiconducting behavior below the so-called Peierls transition to the CDW state, and also in NbSe_3 , which remains metallic due to the partial destruction of the Fermi surface by the charge-density-wave formation.

In this paper we examine the ac properties of a hitherto less intensively studied material, $(\text{NbSe}_4)_2\text{I}$, which undergoes a Peierls transition at $T_p \sim 210$ K.⁵ We find a well-defined pinned-mode resonance centered at $\omega_0/2\pi = 35$ GHz, which can be described by an enormous effective mass $m^*/m_e \sim 10^4$ (where m_e is the free-electron mass) and a strongly temperature-dependent damping constant τ^* . The maximum conductivity, given by $\sigma_{\text{CDW}} = ne^2\tau^*/m^*$, where n is the number of electrons condensed in the CDW state, is close to the conductivity which would be observed in the absence of the Peierls transition, suggesting that $\tau^*/m^* \sim \tau/m$, where τ and m refer to the relaxation time and band mass for the single-

particle conduction process. The conductivity measured in the radiofrequency spectral range is not in agreement with the parameters which characterize the pinned-mode resonance (within the framework of a simple harmonic-oscillator description), and is suggestive for a strongly temperature-dependent long-time tail. The temperature dependence of the low-frequency dielectric constant is also examined and contrasted with the temperature dependence of the pinning frequency and of the threshold field E_T for the onset of nonlinear dc conduction.

In Sec. II, we describe our sample preparation and analysis together with the experimental methods. The experimental results are summarized in Sec. III, while Sec. IV summarizes our analyses. The conclusions are described in Sec. V. Part of our experimental results have been published earlier.⁶

II. EXPERIMENTAL METHODS

In contrast to $(\text{TaSe}_4)_2\text{I}$, the ternary compounds $(\text{NbSe}_4)_x\text{I}$ crystallize with various stoichiometries,⁷ and compounds with $x = 2$,⁵ $3/3$,⁸ and 3 (Ref. 9) have been identified in the literature. The compound $(\text{NbSe}_4)_3\text{I}$ is a semiconductor, and the state appears to be that of a simple band semiconductor with no apparent nonlinear and frequency-dependent response. Both $(\text{NbSe}_4)_2\text{I}$ and $(\text{NbSe}_4)_{3.3}\text{I}$ undergo metal-insulator transitions, the former at $T_p = 210$ K, the latter at $T_p = 270$ K, and both transitions are due to the formation of charge-density waves. The conductivity was found to be nonlinear in both materials below T_p .

$(\text{NbSe}_4)_x\text{I}$ crystals were grown by us using the standard thermal gradient technique, by mixing the appropriate

amount of starting ingredients together and heating them to 800°C (hot end, with the cold end approximately 50°C lower) in a closed capsule. Two visually well-distinguishable types of crystals were formed after a period of a few days. Crystals of type *A* have well-defined three-dimensional character, with typical dimensions of $1 \times 1 \times 10 \text{ mm}^3$. Powder x-ray measurements agree with published data on the $x=3$ compound, and also the dc resistivity, shown in Fig. 1, agrees with experiments reported earlier on this compound. We also recover a sharp phase transition at $T=279 \text{ K}$, as evidenced by the logarithmic derivative, displayed in the inset of Fig. 1. We believe therefore that our crystals of type *A* correspond to $(\text{NbSe}_4)_3\text{I}$. In contrast, some crystals from the same preparation batch (type *B*) are distinctively more fiberlike (similar to TaS_3), and have typical dimensions of $0.1 \times 0.1 \times 5 \text{ mm}^3$. Powder x-ray measurements give reflections which closely correspond to published data on $(\text{NbSe}_4)_2\text{I}$. The dc conductivity, shown in Fig. 2, signals a well-defined phase transition (see the logarithmic derivative in the inset of the figure) at $T=230 \text{ K}$, somewhat above the transition temperature of $T_p=210 \text{ K}$ reported for this compound. We believe therefore that our type-*B* crystals correspond to $(\text{NbSe}_4)_2\text{I}$. The different transition temperature most probably corresponds to a slightly different I composition, and not to substantial disorder (which also would suppress the transition), as the transition is sharp and not significantly smeared, as would be expected for important disorder effects.

The ac response was examined at several distinct frequencies in the micro- and millimeter-wave spectral range. At 9 and 17 GHz, cavity-perturbation techniques were employed,¹⁰ and we used a bridge configuration¹¹ at higher frequencies. Both methods give both $\text{Re}\sigma(\omega)$ and $\text{Im}\sigma(\omega)$, which are extracted from the measured shift and

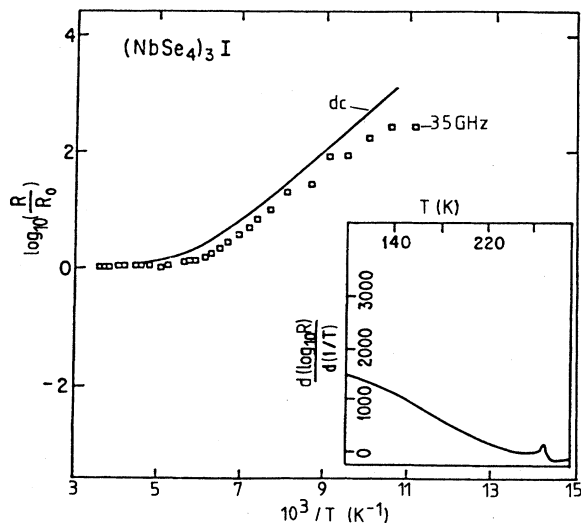


FIG. 1. Temperature dependence of the dc and 35-GHz resistivity of $(\text{NbSe}_4)_3\text{I}$. The inset shows the logarithmic derivative $d(\log_{10}R)/d(1/T)$ vs temperature.

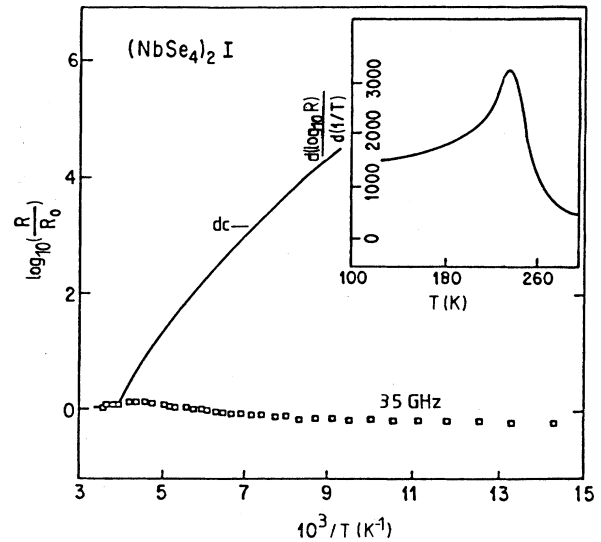


FIG. 2. Temperature dependence of the dc and 35-GHz resistivity of $(\text{NbSe}_4)_2\text{I}$. The inset shows the logarithmic derivative $d(\log_{10}R)/d(1/T)$ vs temperature.

change of absorption in case of cavities, and from the measured attenuation and phase shift in case of bridge-configuration measurements. In the radiofrequency spectral range a Hewlett Packard 8725 network analyzer, operating between 4 and 500 MHz in a continuous-frequency mode, was used. Both the bridge and network-analyzer methods utilize a home-built gas-flow system, which operates in the 20–300-K temperature range, and the cavity-perturbation measurements were performed in conventional He^4 cryostats down to 1.5 K.

III. EXPERIMENTAL RESULTS

Figure 3 shows results of measurements of the real part of the conductivity, $\text{Re}\sigma$, normalized to its room-temperature value versus temperature obtained with dc methods (solid curve), network analyzer (0.5 GHz), cavity-perturbation methods (9 and 17 GHz), and microwave bridges (35, 60, and 94 GHz). The conductivity was found to be frequency independent within the experimental error of approximately 20%, well above the transition temperature. While the behavior is semiconductor like at frequencies well below or above 35 GHz at temperatures below T_p , the metal-semiconductor transition is wiped out for frequencies ranging from approximately 30 to 60 GHz. Below T_p , at 35 GHz the conductivity reaches values up to a factor of 3 higher than the room-temperature value, while the dc conductivity decreases by 5 orders of magnitude between T_p and 100 K.

The temperature dependence of the dielectric constant ϵ calculated from the imaginary part of the conductivity, $\text{Im}\sigma$, is displayed for several frequencies in Fig. 4. This dependence shows three essential features. First, ϵ is

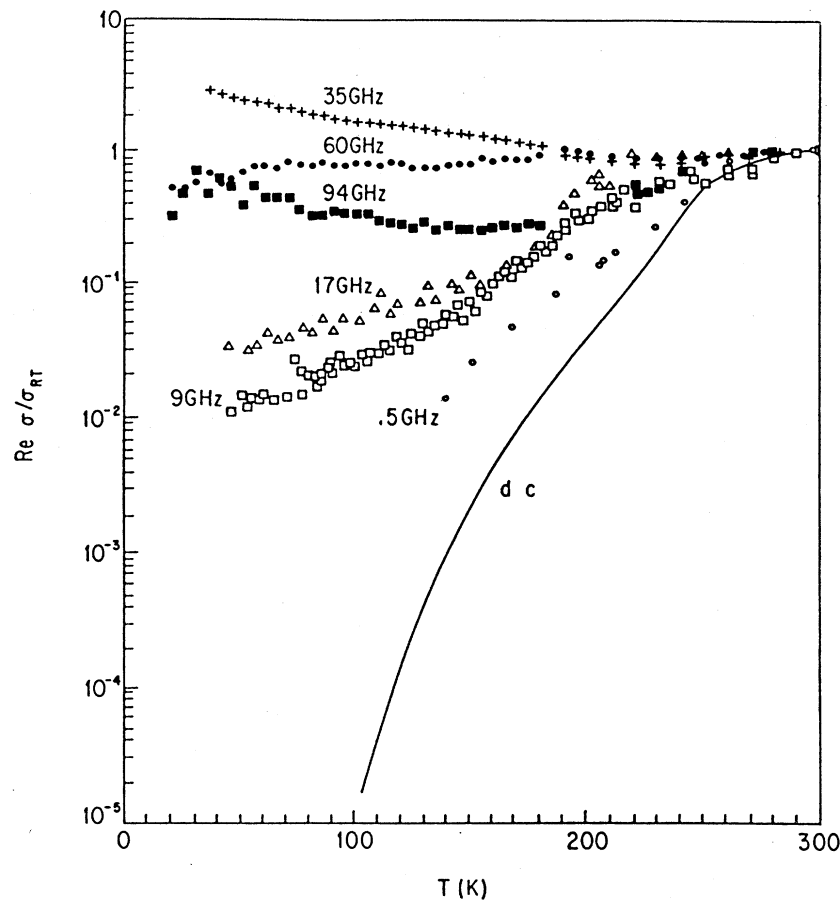


FIG. 3. Temperature dependence of the conductivity of $(\text{NbSe}_4)_2\text{I}$ at different frequencies.

rather small at $\omega/2\pi=35$ GHz, where there is a peak in the real part of conductivity. The maximum value of about 3.5×10^4 is nevertheless much smaller than, for example, in NbSe_3 , where values up to 10^9 were reported.¹ Second, at frequencies above 35 GHz, the dielectric constant is negative, with absolute values which increase monotonically with decreasing temperatures and which are typically 1 order of magnitude smaller than those for frequencies below 35 GHz. Third, ϵ is zero above T_p , as expected for a metal.

The conductivity calculated from the reflection coefficient measured in the radiofrequency range from 4 to 600 MHz with a HP network analyzer is plotted as a function of frequency in Fig. 5 for a temperature of 170 K. The overall features are the same for all temperatures below T_p , while the frequency-dependent contribution to the conductivity disappears more or less abruptly above this temperature. In the low-frequency range up to 10–70 MHz some uncertainty may arise from the subtraction of the Ohmic part of the conductivity measured with a different setup; at higher frequencies this error becomes negligible. The real part of the CDW conductivity, shown in the upper part of Fig. 5, as well as the imaginary part, shown in the lower part, shows a linear

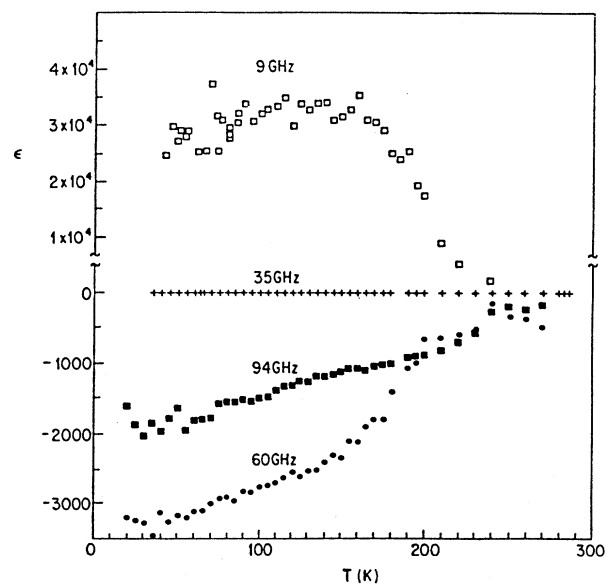


FIG. 4. Temperature dependence of the dielectric constant of $(\text{NbSe}_4)_2\text{I}$ at various frequencies.

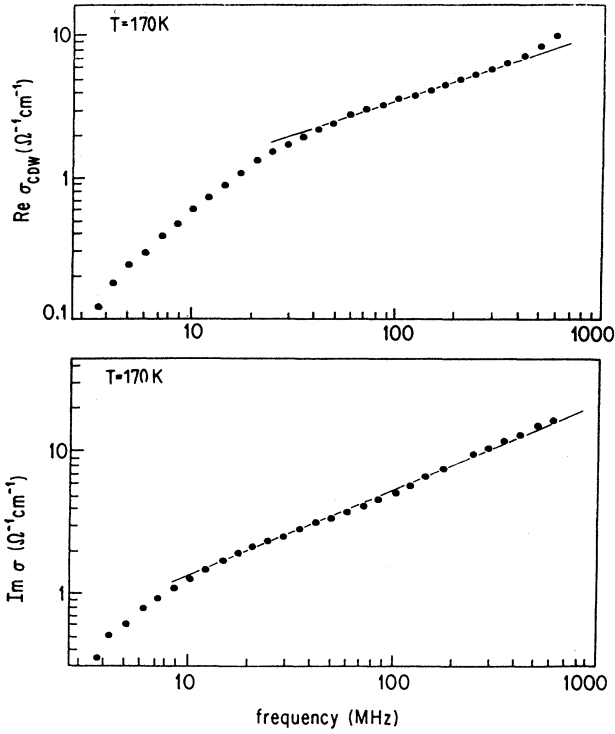


FIG. 5. Frequency dependence of $\text{Re}\sigma(\omega)$ and $\text{Im}\sigma(\omega)$ in the radiofrequency spectral range at $T = 170$ K.

behavior in a log-log plot, indicating a ω^α law, $\sigma(\omega) = A(i\omega/\omega_0)^\alpha$, with $\alpha < 1$, at least above 20 MHz.

IV. DISCUSSION

We first note that the overall behavior observed is rather similar to that found for $(\text{TaSe}_4)_2\text{I}$ (Ref. 3) (although the dielectric constant has not been reported on this latter compound). The overall similarity is quite remarkable, particularly because the details of the ω -dependent response are determined by factors like the residual impurity concentration, not expected to be the same in the two materials. However, the absence of enhanced ac response in $(\text{NbSe}_4)_3\text{I}$, as shown in Fig. 1 together with the results reported in Figs. 3 and 4, clearly demonstrates that $\sigma(\omega)$ observed below the single-particle energies is associated with the charge-density-wave ground state. Consequently, we believe that our measurements reflect the dynamics of the collective mode.

One of the fundamental characteristics of charge-density-wave dynamics is the strongly frequency-dependent response at frequencies well below those which correspond to the single-particle gap Δ .¹ The mode can be represented by an effective mass¹²

$$\frac{m^*}{m} = 1 + \frac{4\Delta^2}{\lambda\omega_{2k_F}^2}, \quad (1)$$

where λ is the electron-phonon coupling constant, and

ω_{2k_F} is the phonon frequency at wave vector $q = 2k_F$, by a so-called pinning frequency ω_0 describing the interaction between the collective CDW mode and impurities, and by a phenomenological damping constant τ^* . In terms of a classical description the equation of motion is

$$\frac{d^2x}{dt^2} + \frac{1}{\tau^*} \frac{dx}{dt} + \omega_0^2 x = \frac{eE(\omega)}{m^*}, \quad (2)$$

where x denotes the center-of-mass coordinate of the collective mode and E the applied ac field. Such a description has been applied to describe the frequency-dependent response of the model compounds NbSe_3 , TaS_3 , and $(\text{TaSe}_4)_2\text{I}$.^{3,4} While τ^* and ω_0 are phenomenological parameters, and consequently their magnitude and temperature dependence cannot be directly compared with theory [Eq. (1)], in particular the relation between m^* and Δ has been confirmed by an experiment on the above materials.³ It has, however, been shown¹³ that Δ is much larger in NbSe_3 than that value inferred from the mean-field relation between the single-particle gap and the transition temperature T_P , and also an unusual phonon mode was found¹⁴ by neutron scattering in $(\text{TaSe}_4)_2\text{I}$ at energies corresponding to the pinned-mode energy $\hbar\omega_0$, prompting speculation that the weakly damped ac response at millimeter-wave frequencies is not related to the CDW mode.

In $(\text{NbSe}_4)_2\text{I}$ we find an underdamped ac response, the main characteristics of which can, at least at not too low temperatures, be described in terms of Eq. (2). The description also leads to a large effective mass m^* , in accordance with Eq. (1). Our observation reinforces the earlier conclusion that $\sigma(\omega)$ in these compounds is due to the collective response of the pinned charge-density-wave mode.

In order to characterize the collective-mode response we have used Eq. (2) to describe both $\text{Re}\sigma(\omega)$ and $\text{Im}\sigma(\omega)$ at certain selected temperatures. Fits to Eq. (2) are displayed in Fig. 6, with the temperature dependence of the parameters which enter into Eq. (3), m^*/m , ω_0 , and $1/2\pi\tau^*$, shown in Fig. 7.

We first note that the harmonic-oscillator response gives an excellent overall description of both $\text{Re}\sigma(\omega)$ and $\text{Im}\sigma(\omega)$ at temperatures not far below the Peierls transition, a feature also noted in $(\text{TaSe}_4)_2\text{I}$. Also, in $(\text{NbSe}_4)_2\text{I}$, the response is weakly damped, and $\omega_0\tau \sim 1$ in this temperature range. However, the experimentally determined values of $\text{Im}\sigma(\omega)$ at 9 and 17 GHz are by a factor of 3–4 higher than the values given by the single-oscillator model,

$$\sigma_{\text{CDW}}(\omega) = \frac{ne^2\tau^*}{m^*} \frac{i\omega/\tau^*}{(\omega_0^2 - \omega^2) + i\omega/\tau^*}, \quad (3)$$

using the same parameters ω_0 and τ^* as obtained from a fit to $\text{Re}\sigma(\omega)$. The description gets progressively less appropriate when the temperature decreases, and at low temperatures it is evident that $\sigma(\omega)$ cannot be described in terms of a single-degree-of-freedom harmonic-oscillator response. Another observation relevant to that made above is also clear in Fig. 3: while the high-frequency response is only weakly temperature depen-

dent, the response at low frequencies (below 30 GHz) progressively freezes out with decreasing temperature. This feature has recently been suggested¹⁵ to be the consequence of the dynamics of the internal degrees of freedom: disorder due to randomly distributed impurities leads to a “glassy” behavior, with low-frequency behavior characterized by the buildup of internal polarizations. These in turn have to be screened by uncondensed electrons; hence the response is strongly temperature dependent. In contrast, at high frequencies such internal polarization effects have less importance.

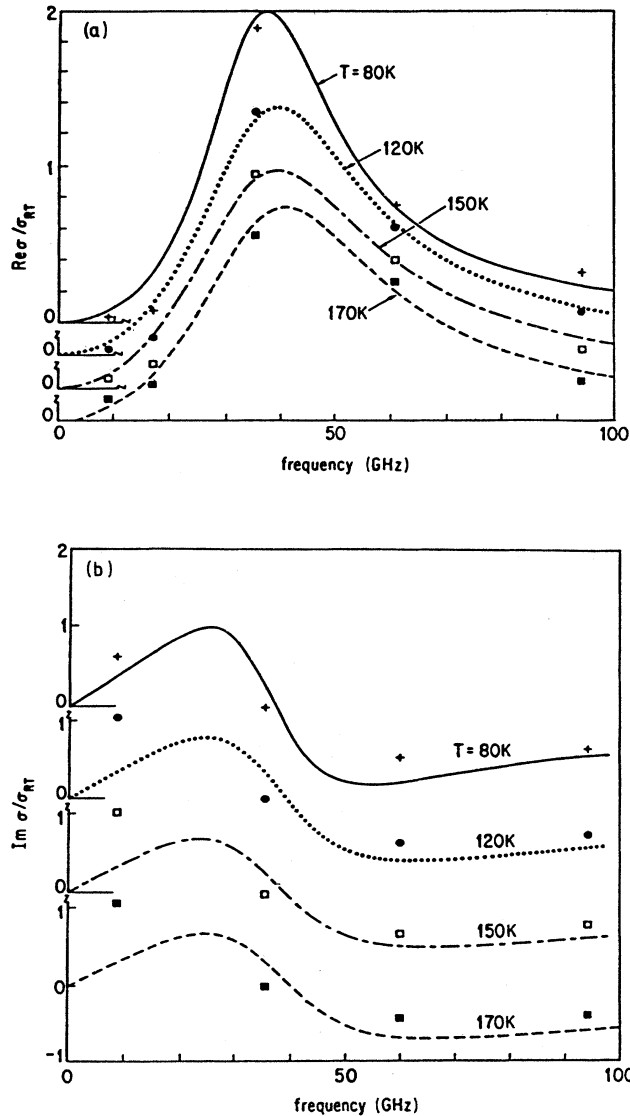


FIG. 6. (a) $\text{Re}\sigma(\omega)$ vs frequency at various temperatures. The solid, dotted, dashed-dotted, and dashed lines are fits to a harmonic-oscillator response, with parameters given in Fig. 7. (b) $\text{Im}\sigma(\omega)$ vs frequency at various temperatures. The solid, dotted, dashed-dotted, and dashed lines are fits to a harmonic-oscillator response, with parameters given in Fig. 7.

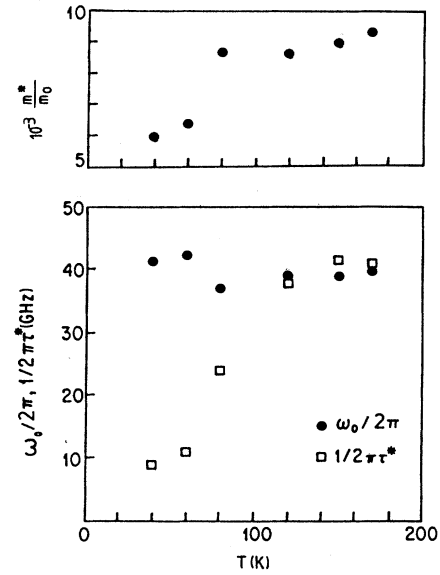


FIG. 7. Temperature dependence of the effective mass, pinning frequency, and damping constant.

The parameters, which are described by fitting the experimental results to Eq. (3), are displayed in Fig. 7. In contrast to the results in TaS_3 ,² and in NbSe_3 , the damping frequency $1/2\pi\tau^*$ observed here depends strongly on temperature below approximately 130 K, while it tends to saturate at higher temperatures as $T \rightarrow T_p$. We note that the theory of CDW damping by Takada, Wong, and Holstein,¹⁶ which assumes scattering with thermally ambient phasons as the predominant mechanism for CDW damping, predicts that $1/\tau^* \sim T^2$, in fair qualitative agreement with our experimental results. In the absence of detailed knowledge of the parameters which enter in the relation, we cannot make a direct comparison between the coefficient measured and calculated by Takada *et al.*¹⁶

The pinning frequency ω_0 is found to be independent of temperature, and its value of approximately 40 GHz is comparable to the one found in $(\text{TaSe}_4)_2\text{I}$.³ It is somewhat surprising that different materials show similar pinning frequencies, which are most probably determined by residual impurities in the specimens. In NbSe_3 and in $(\text{TaSe}_4)_2\text{I}$ doped with Nb impurities, the pinning frequency is strongly impurity dependent. Similar studies on the material $(\text{NbSe}_4)_2\text{I}$ could further clarify the role of impurities. For the calculation of the effective mass m^* from σ_{max} and τ^* , we assumed³ the same carrier concentration ($n_{\text{CDW}} = 1.7 \times 10^{21} \text{ cm}^{-3}$) as in $(\text{TaSe}_4)_2\text{I}$. This again leads to a similar ratio of m^*/m_e , where m_e is the free-electron mass in both materials, with a value of 9300 at 170 K in the Nb compound. Although m^*/m_e shows a decrease with decreasing temperature to a value of 6000 at 40 K, below about 100 K the fit to a single harmonic-oscillator response gets progressively worse, and we believe that the temperature dependence of m^* below 100

K is of spurious origin. We also note that mean-field theory predicts the ratio of $m^*(T)/n(T)$ to be temperature independent;¹⁶ a determination of $n(T)$ would be necessary to clarify whether this is the case. We expect, however, that because of strong fluctuation effects above the Peierls transition (brought about by one-dimensional effects),¹⁷ the order parameter should be well developed at T_p , with little temperature dependence of Δ below the transition. Thus, our finding strongly supports the conjecture that $m^*(T)/n(T)$ is independent of temperature.

While the conductivity can, in the micro- and millimeter-wave spectral range, be described with a harmonic-oscillator response with parameters ω_0 , $1/\tau^*$, and m^* , which are only weakly temperature dependent, experiments well below the pinning frequency clearly demonstrate the breakdown of such an approach. In the low-frequency $\omega \ll \omega_0$ limit, the ac response of a harmonic oscillator is given by

$$\text{Re}\sigma(\omega) = A\omega^2, \quad \text{Im}\sigma(\omega) = B\omega, \quad (4)$$

in clear disagreement with the experimental results displayed in Fig. 5. In this spectral range, our experiments are in broad qualitative agreement with results obtained in $\text{K}_{0.3}\text{MoO}_3$,¹⁸ TaS_3 ,¹⁹ and $(\text{TaSe}_4)_2\text{I}$,²⁰ and show a rather weak (sublinear) frequency dependence. Experimental results obtained in the above materials can be well described by empirical expressions, such as the Cole-Cole or Cole-Davidson formula, which suggest a broad distribution of relaxation times and/or pinning frequencies, or alternatively—over a limited frequency range—by

$$\sigma(\omega) = A \left[\frac{i\omega}{\omega_0} \right]^\alpha, \quad (5)$$

with $\alpha < 1$. Such fractional power-law dependence has been found in many materials²¹ where disorder plays an important role, and has been consequently used to argue that disorder effects are important in the dynamics of charge-density waves. The experimental results of Fig. 5 can also be adequately described by Eq. (5), and the solid lines give $\alpha = 0.8$. It is also evident from the figure that a fractional power-law behavior—and also a simple Cole-Cole or Cole-Davidson expression—holds only to first approximation, and both $\text{Re}\sigma$ and $\text{Im}\sigma$ show a well-defined structure around 20 MHz. The situation is similar to that found recently in $\text{K}_{0.3}\text{MoO}_3$,²² and in $(\text{TaSe}_4)_2\text{I}$,²⁰ and will be discussed later.

In contrast to the high-frequency response, the conductivity in the radiofrequency spectral range is also strongly temperature dependent. Both $\text{Re}\sigma(\omega)$ and $\text{Im}\sigma(\omega)$, measured at two different frequencies, are displayed as the function of the inverse temperature in Fig. 8. Both components of the conductivity decrease with decreasing temperature, indicating a progressive freezeout of the low-frequency conductivity. Although our experiments have been confined to a relatively narrow temperature range, in this temperature range the experimental results can be well represented by the expression

$$\sigma(\omega) = A \left[\frac{i\omega}{\omega_0} \right]^\alpha f(T), \quad (6)$$

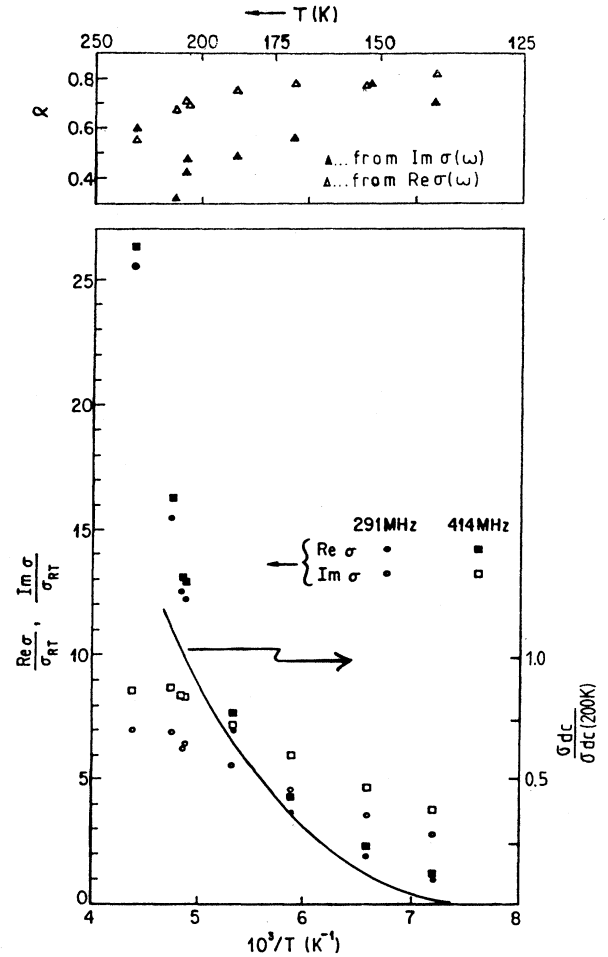


FIG. 8. Temperature dependence of $\text{Re}\sigma(\omega)$ and $\text{Im}\sigma(\omega)$ measured at two different frequencies, and the exponent α , which appears in Eq. (5).

with $f(T)$ close to $\sigma_{\text{dc}}(T)$, the temperature dependence of the low-field dc conductivity. The temperature dependence of the dc conductivity normalized to σ_{dc} at 200 K is shown by the solid line in Fig. 8. We did not conduct experiments over a broad enough frequency range to test whether the approach by Cava *et al.* on the frequency and temperature dependence of the low-frequency response²³ is appropriate to $(\text{NbSe}_4)_2\text{I}$, but our results also are suggestive of low-frequency fluctuations, which are progressively removed from the spectral weight as the temperature is decreased. Thus, our experimental results also support earlier results obtained on the basis of both frequency- and field-dependent conductivity measurements, namely that normal electrons play an important role in the low-frequency CDW response by providing screening for the polarizations which are created by the low-frequency deformations of the collective mode.¹⁵

V. CONCLUSIONS

In this paper we have presented detailed experimental results on the real and imaginary components of the com-

plex conductivity in the material $(\text{NbSe}_4)_2\text{I}$. At high frequencies, in the micro- and millimeter-wave spectral range both components can be analyzed by assuming a harmonic-oscillator response. We find a rather large effective mass $m^*/m_e \simeq 10^4$, which is in agreement with the mean-field theory of Lee, Rice, and Anderson.¹² This value is comparable to that measured in $(\text{TaSe}_4)_2\text{I}$, and is larger than that measured in all other materials with a CDW ground state. This is not surprising, as in both $(\text{TaSe}_4)_2\text{I}$ and $(\text{NbSe}_4)_2\text{I}$ the single-particle gap is significantly larger than in the other materials, and this (within the framework of the mean-field theory) also is suggestive for a larger m^*/m_e for comparable λ and ω_{2k_F} values.

The temperature dependence of the damping constant is also similar to that measured in other materials. The resonance is weakly damped at low temperatures, while it becomes overdamped close to the transition temperature. As discussed earlier, the temperature dependence of the effective mass and damping constant, displayed in Fig. 7, is unexplained at present. We note, however, that the conductivity at resonance $\sigma(\omega=\omega_0)=ne^2\tau^*/m^*$ is close to the value which would be recovered in the absence of a Peierls transition. This is particularly evident from Fig. 3, where conductivity measured at 35 GHz (i.e., close to ω_0) continues to increase with decreasing temperature, in a fashion characteristic of a metallic behavior without a phase transition. This implies that

$$\frac{\tau^*}{m^*} \sim \frac{\tau}{m}, \quad (7)$$

where τ and m refer to single-particle relaxation time and mass, as suggested by Gor'kov and Dolgov²⁴ and recently by Maki and Virosztek.²⁵ Again, the above relation has been found to be valid in TaS_3 ,² and in $(\text{TaSe}_4)_2\text{I}$.²⁶

The pinning frequency ω_0 is also comparable to that measured in other materials, and also in this compound we find ω_0 to be nearly temperature independent. This, within a simple harmonic-oscillator approach, would indicate a temperature-independent low-frequency dielectric constant

$$\epsilon(\omega \rightarrow 0) = 1 + \frac{4\pi ne^2}{m^* \omega_0^2}, \quad (8)$$

with an approximate value (with $n \simeq 10^{21} \text{ cm}^{-3}$, and m^* and ω_0 values determined before) of $\epsilon(\omega \rightarrow 0) \sim 10^4$. As discussed earlier, the dielectric constant measured in the radiofrequency spectral range is significantly larger than this value, and is furthermore strongly temperature dependent. The excess low-frequency spectral response is further demonstrated in Fig. 9, where $\text{Re}\sigma(\omega)$ measured at radiofrequency and micro- and millimeter-wave frequencies is summarized. The solid line in the figure is harmonic-oscillator response, as discussed earlier. The low-frequency tail, which is also strongly temperature dependent, is due to disorder effects. Several models²⁷ have been advanced to account for deviations from a single oscillator response. Some of these assume a broad and smooth distribution of relaxation times and/or pin-

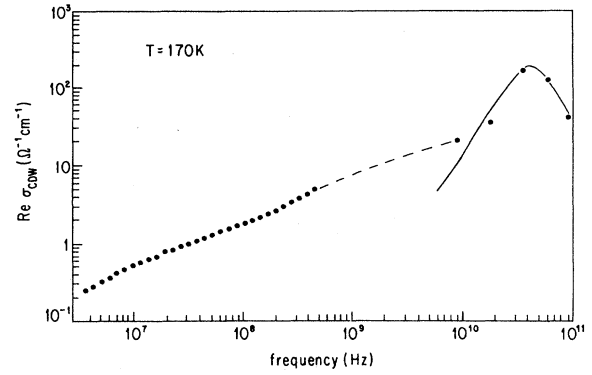


FIG. 9. $\text{Re}\sigma(\omega)$ over a broad frequency scale measured at $T=170$ K. Both the pinned-mode resonance, centered around 35 GHz, and the low-frequency tail are evident in the figure. The solid line is a fit to the harmonic-oscillator response, the dotted line is a guide to the eye.

ning frequencies, while others start from the so-called Fukuyama-Lee-Rice model, where pinning by randomly distributed impurities is explicitly taken into account. None of these models accounts for the essential feature of our experimental results: the well-defined resonance at high frequencies, together with a long-time tail at low frequencies. Two different explanations have been advanced to account for such features of the spectral response. It has been suggested²⁸ that $\sigma(\omega)$ reflects two distinct response phenomena: the ac response of the pinned CDW mode, which oscillates about the equilibrium position at high frequencies, and a tunneling contribution to the frequency-dependent conductivity at low frequencies. The former can be described by standard expressions, such as Eq. (2) for $\text{Re}\sigma(\omega)$ and $\text{Im}\sigma(\omega)$, while for the latter $\sigma(\omega)$ scales²⁹ with the field-dependent conductivity $\sigma(E)$. While we have not conducted detailed experiments on the nonlinear conductivity, experiments in $(\text{TaSe}_4)_2\text{I}$ are suggestive for a rather similar ω - and E -dependent response.³⁰ Alternatively, the behavior has been modeled recently¹⁵ assuming that local deformations of the collective mode are important in the low-frequency response, while they do not play a role at high frequencies. A model which treats both the longitudinal and transverse modes of the ground state leads to a pinned-mode contribution, together with a low-frequency plateau, similar to that observed in Fig. 9.

We have also measured the temperature dependence of the threshold field E_T in an attempt to relate the ω -dependent response to the nonlinear conduction due to charge-density waves. E_T as the function of temperature is displayed in Fig. 10. As in $(\text{TaSe}_4)_2\text{I}$, the threshold field is approximately 1 V/cm, somewhat below the transition temperature, and increases with decreasing temperature. The temperature dependence can be well described by the expression

$$E_T = E_T^0 \exp(-T/T_0), \quad (9)$$

with $T_0 < \Delta$, as suggested by Maki.¹⁷ More importantly,

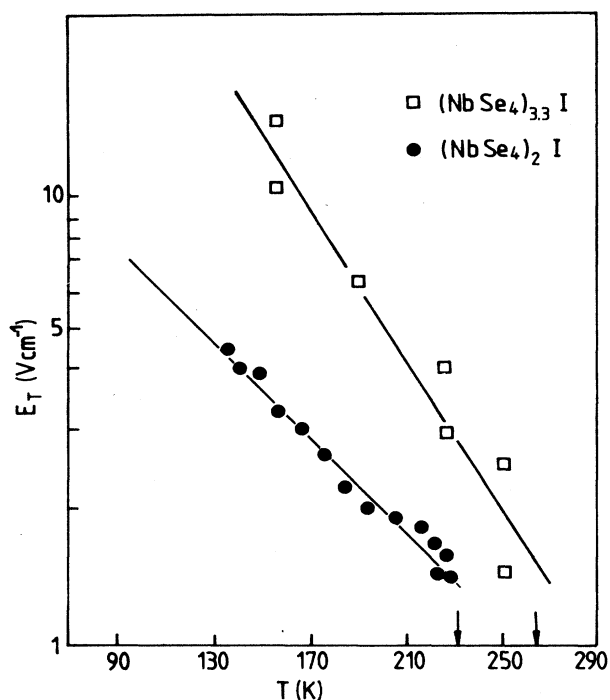


FIG. 10. Temperature dependence of the threshold field E_T in $(\text{NbSe}_4)_2\text{I}$. For comparison, E_T values, measured in $(\text{NbSe}_4)_{3.33}\text{I}$, are also included in the figure.

the temperature dependence of the low-frequency dielectric constant and the temperature dependence of the threshold field go hand in hand with ϵE_T approximately constant. This is evident by comparing Figs. 8 and 10: ϵ ,

measured at 291 MHz, decreases by approximately a factor of 2 going from 200 to 130 K, and the threshold field increases approximately by the same ratio in the same temperature range. Furthermore, ϵE_T , normalized to one chain, gives a value of $\epsilon E_T = 0.6e$, comparable to that measured in other materials,³¹ and in good agreement with the various models which connect the ω -dependent and E -dependent response. In contrast, when both quantities are calculated by using ω_0 as input parameters, orders-of-magnitude disagreement between the measured and calculated values is obtained. The measured low-frequency dielectric constant, when compared with Eq. (2), is too large, as discussed earlier. Within the same model, the threshold field is given by

$$E_T = \frac{m^* \omega_0^2}{2e} \lambda, \quad (10)$$

and $m^* = 10^4 m_e$, $\omega_0/2\pi = 35$ GHz, and $n = 10^{21} \text{ cm}^{-3}$ leads to $E_T \approx 10^3 \text{ V/cm}$, in contrast to the measured values displayed in Fig. 10. Consequently, the depinning and the subsequent nonlinear conduction is related to the low-frequency spectral response of the collective mode, and not to the high-frequency part of the pinned-mode resonance.

ACKNOWLEDGMENTS

Two of us (A.P. and W.M.) were supported by the Fonds zur Förderung der wissenschaftlichen Forschung in Österreich, the Austria-United States of America Cooperative Science Program (Grant No. P5359), and a U.S. National Science Foundation grant.

- ¹See for example, *Charge Density Waves in Solids*, Vol. 217 of *Lecture Notes in Physics*, edited by Gy. Hutiray and J. Solyom (Springer, Berlin, 1985).
- ²S. Sridhar, D. Reagor, and G. Grüner, *Phys. Rev. B* **34**, 2223 (1986).
- ³D. Reagor, S. Sridhar, M. Maki, and G. Grüner, *Phys. Rev. B* **32**, 8445 (1985).
- ⁴G. Mihaly, T. W. Kim, D. Reagor, and G. Grüner (unpublished).
- ⁵H. Fujishita, M. Sato, and S. Hoshino, *Solid State Commun.* **49**, 313 (1984).
- ⁶A. Philipp, W. Mayr, T. W. Kim, and G. Grüner, *Solid State Commun.* **62**, 521 (1987).
- ⁷P. Gressier, A. Meerschaut, L. Guemas, and J. Rouxel, *J. Solid State Chem.* **51**, 141 (1984).
- ⁸P. Monceau, in *Electronic Properties of Inorganic Quasi-1D Compounds*, edited by P. Monceau (Reidel, Dordrecht, 1985).
- ⁹M. Izumi, T. Iwazumi, T. Seino, K. Uchinokura, R. Yoshizaki, and E. Matsuura, *Solid State Commun.* **49**, 423 (1984).
- ¹⁰L. I. Buravov and I. F. Shchegolev, *Prib. Tekh. Eksp.* **14**, 171 (1971).
- ¹¹S. Sridhar, D. Reagor and G. Grüner, *Rev. Sci. Instrum.* **56**, 1946 (1985); Tae Wan Kim, W. P. Beyermann, D. Reagor,

- and G. Grüner, *ibid.* **59**, 1219 (1988).
- ¹²P. A. Lee, T. M. Rice, and P. W. Anderson, *Solid State Commun.* **14**, 703 (1974).
- ¹³W. A. Challener and P. L. Richards, *Solid State Commun.* **52**, 117 (1984).
- ¹⁴P. Monceau, L. Bernard, R. Currat, F. Levy, and J. Rouxel, *Synth. Metals* **19**, 819 (1987).
- ¹⁵P. Littlewood, *Phys. Rev. B* **36**, 3108 (1987).
- ¹⁶S. Takada, K. Y. M. Wong, and T. Holstein, *Phys. Rev. B* **32**, 4639 (1985).
- ¹⁷K. Maki, *Phys. Rev. B* **33**, 2852 (1986).
- ¹⁸R. J. Cava, R. M. Fleming, P. Littlewood, E. A. Rietman, L. F. Schneemeyer, and R. G. Dunn, *Phys. Rev. B* **30**, 3228 (1984).
- ¹⁹W. Y. Wu, L. Mihaly, G. Mozurkewich, and G. Grüner, *Phys. Rev. Lett.* **52**, 2382 (1984).
- ²⁰G. Grüner, D. Reagor, S. E. Brown, and S. Sridhar, *Bull. Am. Phys. Soc.* **31**, 286 (1986).
- ²¹W. Y. Wu, L. Mihaly, G. Mozurkewich, and G. Grüner, *Phys. Rev. B* **33**, 2444 (1986).
- ²²G. Mihaly, T. Chen, T. W. Kim, and G. Grüner, *Phys. Rev. B* **38**, 3602 (1988).
- ²³R. J. Cava, P. Littlewood, R. M. Fleming, R. G. Dunn, and E.

- A. Rietman, Phys. Rev. B **33**, 2439 (1986).
- ²⁴L. P. Gor'kov and E. N. Dolgov, J. Low Temp. Phys. **42**, 101 (1981).
- ²⁵K. Maki and A. Virosztek, Phys. Rev. B **39**, 2511 (1989).
- ²⁶Tae Wan Kim, G. Grüner, K. Maki, and A. Virosztek (unpublished).
- ²⁷M. Bleher and W. Wonneberger, Solid State Commun. **69**, 103 (1989); J. R. Tucker, W. G. Lyons, and G. Gammie, Phys. Rev. B **38**, 1128 (1988).
- ²⁸John Bardeen (private communication).
- ²⁹John Bardeen, Phys. Rev. Lett. **55**, 1010 (1985).
- ³⁰D. Reagor and S. Brown (unpublished).
- ³¹Wei-Yu Wu, A. Jánossy, and G. Grüner, Solid State Commun. **49**, 1013 (1984).